HHS Public Access

Author manuscript

Circ Arrhythm Electrophysiol. Author manuscript; available in PMC 2017 March 01.

Published in final edited form as:

Circ Arrhythm Electrophysiol. 2016 March ; 9(3): e002897. doi:10.1161/CIRCEP.115.002897.

Association of Left Atrial Local Conduction Velocity with Late Gadolinium Enhancement on Cardiac Magnetic Resonance in Patients with Atrial Fibrillation

Kotaro Fukumoto, MD, PhD[1], **Mohammadali Habibi, MD**[1], **Esra Gucuk Ipek, MD**[1], **Sohail Zahid, BS**[2], **Irfan M. Khurram, MD**[1], **Stefan L. Zimmerman, MD**[3], **Vadim Zipunnikov, PhD**[4], **David Spragg, MD**[1], **Hiroshi Ashikaga, MD, PhD**[1,2], **Natalia Trayanova, PhD**[1,2], **Gordon F. Tomaselli, MD**[1], **John Rickard, MD**[1], **Joseph E. Marine, MD**[1], **Ronald D. Berger, MD, PhD**[1,2], **Hugh Calkins, MD**[1], and **Saman Nazarian, MD, PhD**[1,5]

[1]Section of Cardiac Electrophsyiology, Johns Hopkins University, Baltimore, MD

[2]Department of Biomedical Engineering, Johns Hopkins University, Baltimore, MD

[3]Department of Radiology, Johns Hopkins University, Baltimore, MD

[4]Department of Biostatistics, Johns Hopkins University, Baltimore, MD

[5]Department of Epidemiology, Johns Hopkins University, Baltimore, MD

Abstract

Background—Prior studies have demonstrated regional left atrial late gadolinium enhancement (LGE) heterogeneity on magnetic resonance imaging. Heterogeneity in regional conduction velocities is a critical substrate for functional reentry. We sought to examine the association between left atrial conduction velocity and LGE in patients with atrial fibrillation (AF).

Methods and Results—LGE imaging and left atrial activation mapping were performed during sinus rhythm in 22 patients prior to pulmonary vein isolation. The locations of 1468 electroanatomic map points were registered to the corresponding anatomic sites on 469 axial LGE image planes. The local conduction velocity at each point was calculated using previously established methods. The myocardial wall thickness and image intensity ratio (IIR) defined as left atrial myocardial LGE signal intensity divided by the mean left atrial blood pool intensity was calculated for each mapping site. The local conduction velocity and IIR in the left atrium (mean ± standard deviation) were 0.98±0.46 m/sec and 0.95±0.26, respectively. In multivariable regression analysis, clustered by patient, and adjusting for left atrial wall thickness, conduction velocity was associated with the local IIR (0.20 m/sec decrease in conduction velocity per increase in unit IIR, P<0.001).

Correspondence: Saman Nazarian, MD, PhD, Johns Hopkins University, Carnegie 592A, 600 N. Wolfe Street, Baltimore, MD 21287, Tel: 410-614-2751, Fax: 410-502-4854, snazarian@jhmi.edu.

Conflict of Interest Disclosures: Dr. Nazarian is a consultant to Medtronic, CardioSolv, and Biosense-Webster Inc and principal investigator for research funding to Johns Hopkins University from Biosense-Webster Inc.

Conclusions—In this clinical *in vivo* study we demonstrate that left atrial myocardium with increased gadolinium uptake has lower local conduction velocity. Identification of such regions may facilitate the targeting of the substrate for reentrant arrhythmias.

Keywords

conduction velocity; fibrosis; atrial fibrillation; magnetic resonance imaging

Introduction

Regional heterogeneity in left atrial (LA) conduction velocity (CV) is an important substrate for development of functional reentry and atrial fibrillation (AF).[1] Myocardial fibrosis can contribute to decreased regional CV[2–4] and is associated with the initiation and perpetuation of AF.[5–8] Late gadolinium enhancement (LGE) magnetic resonance imaging (MRI)[9, 10] has been proposed as a useful tool for visualization of atrial fibrosis.[11] We have previously reported the association of a normalized parameter, the image intensity ratio (IIR), with local bipolar voltage and established quantitative thresholds of >0.97 and >1.61 corresponding to local bipolar voltage of <0.5 and <0.1mV, respectively.[12] Prior studies have uncovered an association between CV and myocardial fibrosis in the atria of animal models.[2, 4] However, no clinical studies have demonstrated an association between local CV and LA LGE. We sought to investigate the *in vivo* association between local CV during sinus rhythm and myocardial LGE in the human LA.

Methods

Study population

The Johns Hopkins Institutional Review Board approved the study protocol. Written informed consent was obtained from each patient prior to the pre-procedural MRI. Forty-two patients underwent an initial radiofrequency catheter ablation for AF and pre-procedural MRI between December 2011 and March 2013. Twenty patients were excluded due to the presence of AF during electroanatomic mapping (EAM). The remaining 22 patients, who were in sinus rhythm during EAM and MRI, formed the study cohort.

Magnetic resonance imaging

MRI acquisition was performed using a 1.5-Tesla MRI scanner (Avanto, Siemens, Erlangen, Germany). LGE-MRI scans were acquired 17±4.9 (limit 10 to 27) minutes following 0.2 mmol/kg gadolinium injection (gadopentetate dimeglumine: Bayer Healthcare Pharmaceuticals, Montville, NJ) using a fat-saturated three-dimensional IR-prepared fast spoiled gradient recalled echo sequence with respiratory navigation and electrocardigram-gating, echo time of 1.52ms, repetition time of 3.8ms, in-plane resolution of 1.3×1.3, slice thickness of 2.0mm, and flip angle of 10 degrees. Trigger time for three-dimensional LGE-MRI images was optimized to acquire imaging data during ventricular diastole as dictated by inspection of the cine images. The optimal inversion time (TI) was identified with a TI scout scan (median 270 ms, limit 240–290 ms) to maximize nulling of LA myocardium.

Image analysis

QMass MR software (version 7.2, Leiden University Medical Center, Leiden, The Netherlands) was used to quantify scar extent on preoperative LGE-MRI by an observer that was masked to EAM results. Epicardial and endocardial contours were manually drawn around the LA myocardium on axial LGE-MRI planes (Figure 1A). The anatomical reference point was set at the LA posteroseptum, and the LA myocardium in each axial plane was divided into 20 sectors. The IIR for each sector, defined as the mean pixel intensity of each sector divided by the mean pixel intensity of the entire LA blood pool, was calculated. Based upon our prior data that examined the association of IIR with voltage mapping, image sectors with IIR>0.97 were considered enhanced.[12] The average LA wall thickness of each sector was calculated using QMass MR.

Electroanatomic mapping

Prior to radiofrequency ablation, LA activation mapping was performed during sinus rhythm using an EAM system (CARTO3, Biosense Webster, Diamond Bar, CA) and a mapping catheter with a 3.5-mm distal tip (Navistar Thermocool, Biosense Webster). Endocardial contact during point acquisition was validated by recording of a stable contact signal for >2 beats. Three-dimensional position coordinates and local electrograms of all mapping sites were recorded on CARTO. The timing reference for activation mapping was set as a stable coronary sinus electrogram. The local activation time (LAT) of each EAM point was annotated. EAM points recorded during ectopic beats with different intracardiac sequences or different P wave morphologies in surface electrocardiograms from those of sinus rhythm were excluded. If necessary, points were excluded by an observer that was masked to imaging data and prior to registration of EAM to images. Patients were observed for 24 hours following the procedure. No immediate postoperative complications were noted.

Local conduction velocity analysis

The local CV for each point was calculated according to previously established methodology from prior studies.[13–16] The local CV of each EAM point was defined as the average of the CV between that point and 5 adjacent points along the activation front, where the CV between each pair of points was defined as the linear distance between the points divided by the difference in activation times. To avoid the inclusion of CV measurements in a different direction than that of activation propagation, points with difference in local activation time <5 ms from the index point were excluded from the CV calculation for that index point. Using this methodology the CV at all EAM points was automatically calculated with a custom calculating script written in Python (https://www.python.org).

Registration of EAM data and MRI

By using previously validated custom software (Volley, Johns Hopkins University, Baltimore, MD)[12, 17–19] the coordinates of activation map points on EAM were registered to the pre-procedural LGE-MRI axial planes (Figure 1B). The IIR and LA wall thickness of LGE image sectors that corresponded to each EAM point were measured.

Statistical analyses

Continuous variables are expressed as mean ± standard deviation (SD) and categorical data as numbers or percentages. The multivariable association of CV as dependent variable with IIR and thickness as independent variables was assessed using a multi-level multivariable regression model, clustered by patient. The multilevel model approach utilized here recognizes the existence of data clustering by allowing for patient-specific intercepts and slopes. Failure to account for data clustering and the between-patient variability in slopes and intercepts can result in incorrect inferences and overstatement of statistical significance. The possibility of multiplicative interaction between our main effect variable (IIR) and AF type was explored by subsequent addition of a multiplicative term, followed by stratification by AF type. To validate the reliability of our custom script for automated calculation of local CV, the automated results were compared to results from manual calculation using previously reported methodology,[13–16] in a randomly selected sample of 5 patients (434 points). Inter- and intra-observer variability in measuring the IIR and wall thickness were also assessed by repeat review by a second reviewer and repeat review by the original reviewer, in a randomly selected sample of 5 patients. The intra-class correlation coefficients for automatic versus manual CV measurements, and inter- and intra-observer variability of IIR and wall thickness were calculated using two-way random effects models. Statistical analyses were performed using STATA (version 12, StataCorp, College Station, TX).

Results

Patient characteristics

Twenty-two patients (17 males, age 62±9.0 years, 13 paroxysmal, 9 persistent AF) were enrolled in this study. The mean left ventricular ejection fraction was 61±4.2 % (limit 55–68) and the mean CHA_2DS_2-VASc score was 1.9±1.8 (limit 0–6). The participant characteristics have been summarized in Table 1.

Conduction velocity analyses

A total of 2824 points were acquired on EAM of 22 patients. Of all points, 1356 were excluded due to catheter instability or ectopic beats during point acquisition, and the remaining 1468 points (67±30 points-per-patient) were included for local CV calculation. The mean local CV was 0.98±0.46 m/sec (CV limit 0.05–3.22 m/sec, 0.24 between patient and 0.40 within patient SD).

EAM Co-registration and analysis of LGE-MRI

Three-dimensional LGE-MRI with minimal artifacts was obtained in all 22 patients. A total of 9380 image sectors from 469 axial image planes were analyzed. The coordinates of all 1468 EAM points were registered to the LGE-MRI. The mean value of IIR and LA wall thickness of corresponding points were 0.95±0.26 (IIR limit 0.21–2.24, 0.14 between patient and 0.22 within patient SD) and 1.9±0.5mm (thickness limit 0.40–3.63 mm, 0.31 between patient and 0.39 within patient SD), respectively. Figure 2 illustrates the activation propagation, local CV, IIR, and wall thickness in the LA in a representative case. In all

patients, the LA posterior wall adjacent to the left pulmonary vein antra (septo-pulmonary bundle region) had lower local CV and higher IIR compared to other LA sites.

In multi-level multivariable linear regression analyses, clustered by patient, CV was associated with the local IIR (0.20 m/sec decrease in CV per unit increase in IIR, P<0.001) after adjusting for LA wall thickness (0.03 m/sec decrease in CV per mm increase in wall thickness, P=0.33).

When adding EAM point localization in the left LA posterior wall to the regression model, to adjust for the potential confounding effect of myocardial fiber orientation, both the IIR (0.10 m/sec decrease in CV per unit increase in IIR, P=0.044) and left posterior LA localization (0.20 m/sec decrease in CV, P<0.001) remained associated with CV after adjusting for LA wall thickness (0.01 m/sec decrease in CV per mm increase in wall thickness, P=0.58).

We observed the presence of multiplicative interaction between IIR and AF type in their association with CV (Figure 3, P=0.002). After stratification by AF type, the magnitude of association between IIR and CV was higher in the setting of persistent AF (0.34 m/sec decrease in CV per unit increase in IIR, P<0.001). Among the subgroup of patients with paroxysmal AF there was no statistically significant association between IIR and CV (P=0.47).

Validation of automated calculation of local CV

In a randomly selected sample of 5 patients (434 EAM points), the automated results were similar to results from manual calculation. The intra-class correlation coefficient for the reliability of automatic observations versus manual measurements was 0.93.

Inter- and intra-observer variability

For the assessment of inter- and intra-observer variability, repeat analyses by the same observer and the second observer were performed. A total of 407 EAM points and 2280 image sectors on 114 axial MRI planes from a randomly selected sample of 5 patients were analyzed. The intra-class correlation coefficients for intra-observer variability of the IIR and wall thickness were 0.99 and 0.92, respectively. The intra-class correlation coefficients for inter-observer variability of the IIR and wall thickness were 0.98 and 0.69, respectively.

Discussion

Major findings

The major finding of our study is that LA myocardium with increased gadolinium uptake, indicating increased extracellular volume content and slower contrast washout, exhibits lower local CV.

Myocardial fibrosis and conduction velocity

AF facilitates the expression of extracellular matrix proteins in the atrial myocardial tissue and promotes atrial fibrosis.[8, 20] Additional stimuli such as mechanical stress, high rate cell

depolarization, hypoxia, inflammation, and humoral factors also induce cardiac fibroblasts to proliferate and undergo phenotype-change into myofibroblasts, which stimulate other fibroblasts and exacerbate myocardial fibrosis by producing cytokines, growth factors, and extracellular matrix proteins.[21–23] Myocardial fibrosis, in turn, causes decreased CV and regional conduction block, which promote function reentry.[2, 24] Interestingly, factors other than lack of conduction by fibroblasts may explain decreased CV in fibrotic regions. Some evidence suggests that myocytes might form electrical connections with fibroblasts[3, 5, 23, 25] and myofibroblasts[21] through gap junctions. Heterogeneous cell-couplings have been shown to cause conduction slowing and/or excitation failure in cellular models[25] and computer simulations.[26]

In the present study, we demonstrated that LA myocardium with increased LGE intensity has lower local CV compared to unenhanced areas. LA myocardium with fibrosis, or increased myofibroblast content exhibits increased extracellular volume and prolonged contrast retention. The finding that LA regions with LGE conduct slowly provides additional evidence to validate the utility of LGE and particularly IIR as a methodology for LA myocardial characterization, and also suggests a mechanism for the observation that increased pre-existing LGE associates with persistent and recurrent AF.[11] Importantly, in our study, statistical interaction between IIR and AF type was noted in their association with CV. The association of IIR with CV was accentuated in patients with persistent AF. In contrast, while the direction of association was consistent, the magnitude of association was lower and statistical significance was absent in the subgroup with paroxysmal AF. This may be due to progressive structural and electrophysiological remodeling in patients with more advanced arrhythmia.

In seeming contrast to our results, Krul et al[27] reported that local longitudinal CV was faster in *ex vivo* perfused LA appendage specimens with thicker collagen bundles. In their study, the local CV was measured as the slope of the steepest upstroke of the action potential at each pixel of optical mapping. When examining conduction in larger regions more comparable to the scale of analysis in our *in vivo* study, the authors noted activation delay in preparations with a high amount of collagen due to areas of activation block and zig-zag conduction. Thus, the primary difference between our results is likely a matter of scale regarding “local” CV. The different results may also be related to *in vivo* versus *ex vivo* perfused myocardial conditions, LA myocardial versus LA appendage conduction properties, and endocardial versus epicardial CV measurements.

Myocardial fiber orientation and electrical conduction

Myocardial fiber architecture plays a prominent role in electrical propagation.[28–31] Consistent with De Ponti and colleagues’ contact mapping results, we found that the earliest activation site within the LA is the antero-superior breakthrough, which reflects conduction via Bachmann's bundle.[32]

In this study, left posterior LA CV was significantly lower than that of other LA areas. Myofibers of the left posterior LA (septo-pulmonary bundle) descend the posterior wall in a cranio-caudal direction whereas the antral myocardium continuing into the muscular sleeves on the left pulmonary veins are different.[29, 33, 34] These anatomical factors may contribute to

the lower local CV in those regions. Increased extracellular volume (likely due to fibrosis) may also be responsible for the decreased local CV in the left posterior LA because the IIR in that region was higher than that of other LA areas. Importantly, in the present study, localization in the left posterior LA, as well as IIR, were associated with CV. We used localization in the left posterior LA (septo-pulmonary bundle) as a surrogate of fiber orientation because current MRI resolution does not allow direct measurement of fiber orientation. Recently, Poveda et al succeeded in visualization of ventricular myocardial fiber architecture in the canine myocardium by using diffusion tensor MRI and tracography reconstruction.[35] Future MRI developments may enable advanced investigation of LA myofiber orientation and refine our results.

Limitations

This is a relatively small study and future studies with larger patient numbers and denser EAM may allow adjustment for other patient level confounders, which were not analyzed in this study. Mapping point density was reduced due to exclusion of points without a clear contact signal and with evidence of ectopic activation. The routine use of force-sensing catheters will likely improve map density and reduce the propensity for bias. The CMR in-plane image resolution was 1.3 × 1.3 mm. In this study, 9.2% of analyzed LA myocardium appeared less than 1.3 mm thick; thus atrial wall thickness was below the limit of image resolution in some regions. The analyzed LA wall bounded by endocardial and epicardial contours may therefore have included blood pool or epicardial fat in some cases, thus confounding thickness and IIR measurements in thin tissue. Importantly, IIR remained associated with CV (0.16 m/sec decrease in CV per unit increase in IIR, P=0.002) in a sensitivity analysis that excluded regions with tissue thickness <1.3 mm. Our results may be limited by a possibility for positional errors when registering EAM points to corresponding sectors on LGE-MRI based on the registration information obtained by the EAM software. Although we have attempted to adjust for regional differences in CV in multivariable models, some unmeasured confounding likely exists. Based upon the intra-class correlation coefficient of the model, 24% of the total variance in CV is due to differences between patients, with the remaining 76% attributable to within person differences. Factors other than IIR, such as direction of propagation, wave curvature, multiple endocardial breakthroughs, wave collision, and regional differences in myofiber structure and electrophysiological heterogeneity likely drive a significant proportion of the between and within patient variance in CV. In 4 patients we collected data regarding the direction of propagation during sinus rhythm and pacing from the lateral LA. In this underpowered sub-group with 436 mapping points, which adjusted for direction of propagation, a trend for association (consistent with the overall model) was noted between LA LGE and CV (-0.074 m/sec, P=0.16).

Conclusions

Local *in vivo* conduction velocity measurements in the human LA are inversely associated with the IIR, a normalized measure of LGE-MRI intensity. This study provides further validation for the utility of LA LGE for mechanistic studies of the substrate for arrhythmia. Additionally, non-invasive identification of regions with LGE may facilitate the localization

of slow conduction zones as optimal targets for ablation in patients with reentrant tachyarrhythmias.

Acknowledgments

Funding Sources: The study was funded by a Biosense-Webster grant and NIH grants K23HL089333 and R01HL116280 to Dr. Nazarian, the Dr. Francis P. Chiaramonte Foundation, The Norbert and Louise Grunwald Cardiac Arrhythmia Fund, the Marv Weiner Cardiac Arrhythmia Fund, and the Marilyn and Christian Poindexter Research Fund. The content is solely the responsibility of the authors and does not necessarily represent the official views of the NIH.

References

1. Nattel S, Shiroshita-Takeshita A, Brundel BJ, Rivard L. Mechanisms of atrial fibrillation: lessons from animal models. Prog Cardiovasc Dis. 2005; 48:9–28. [PubMed: 16194689]
2. Burstein B, Comtois P, Michael G, Nishida K, Villeneuve L, Yeh YH, Nattel S. Changes in connexin expression and the atrial fibrillation substrate in congestive heart failure. Circ Res. 2009; 105:1213–1222. [PubMed: 19875729]
3. King JH, Huang CL, Fraser JA. Determinants of myocardial conduction velocity: implications for arrhythmogenesis. Front Physiol. 2013; 4:154. [PubMed: 23825462]
4. Li D, Fareh S, Leung TK, Nattel S. Promotion of atrial fibrillation by heart failure in dogs: atrial remodeling of a different sort. Circulation. 1999; 100:87–95. [PubMed: 10393686]
5. Burstein B, Nattel S. Atrial fibrosis: mechanisms and clinical relevance in atrial fibrillation. J Am Coll Cardiol. 2008; 51:802–809. [PubMed: 18294563]
6. Corradi D. Atrial fibrillation from the pathologist's perspective. Cardiovasc Pathol. 2014; 23:71–84. [PubMed: 24462196]
7. Frustaci A, Chimenti C, Bellocci F, Morgante E, Russo MA, Maseri A. Histological substrate of atrial biopsies in patients with lone atrial fibrillation. Circulation. 1997; 96:1180–1184. [PubMed: 9286947]
8. Lin CS, Lai LP, Lin JL, Sun YL, Hsu CW, Chen CL, Mao SJ, Huang SK. Increased expression of extracellular matrix proteins in rapid atrial pacing-induced atrial fibrillation. Heart Rhythm. 2007; 4:938–949. [PubMed: 17599682]
9. Kim RJ, Fieno DS, Parrish TB, Harris K, Chen EL, Simonetti O, Bundy J, Finn JP, Klocke FJ, Judd RM. Relationship of MRI delayed contrast enhancement to irreversible injury, infarct age, and contractile function. Circulation. 1999; 100:1992–2002. [PubMed: 10556226]
10. Rochitte CE, Tassi EM, Shiozaki AA. The emerging role of MRI in the diagnosis and management of cardiomyopathies. Curr Cardiol Rep. 2006; 8:44–52. [PubMed: 16507236]
11. Oakes RS, Badger TJ, Kholmovski EG, Akoum N, Burgon NS, Fish EN, Blauer JJ, Rao SN, DiBella EV, Segerson NM, Daccarett M, Windfelder J, McGann CJ, Parker D, MacLeod RS, Marrouche NF. Detection and quantification of left atrial structural remodeling with delayed-enhancement magnetic resonance imaging in patients with atrial fibrillation. Circulation. 2009; 119:1758–1767. [PubMed: 19307477]
12. Khurram IM, Beinart R, Zipunnikov V, Dewire J, Yarmohammadi H, Sasaki T, Spragg DD, Marine JE, Berger RD, Halperin HR, Calkins H, Zimmerman SL, Nazarian S. Magnetic resonance image intensity ratio, a normalized measure to enable interpatient comparability of left atrial fibrosis. Heart Rhythm. 2014; 11:85–92. [PubMed: 24096166]
13. John B, Stiles MK, Kuklik P, Chandy ST, Young GD, Mackenzie L, Szumowski L, Joseph G, Jose J, Worthley SG, Kalman JM, Sanders P. Electrical remodelling of the left and right atria due to rheumatic mitral stenosis. Eur Heart J. 2008; 29:2234–2243. [PubMed: 18621772]
14. Kistler PM, Sanders P, Fynn SP, Stevenson IH, Spence SJ, Vohra JK, Sparks PB, Kalman JM. Electrophysiologic and electroanatomic changes in the human atrium associated with age. J Am Coll Cardiol. 2004; 44:109–116. [PubMed: 15234418]

15. Miyamoto K, Tsuchiya T, Narita S, Yamaguchi T, Nagamoto Y, Ando S, Hayashida K, Tanioka Y, Takahashi N. Bipolar electrogram amplitudes in the left atrium are related to local conduction velocity in patients with atrial fibrillation. Europace. 2009; 11:1597–1605. [PubMed: 19910315]
16. Sanders P, Morton JB, Kistler PM, Spence SJ, Davidson NC, Hussin A, Vohra JK, Sparks PB, Kalman JM. Electrophysiological and electroanatomic characterization of the atria in sinus node disease: evidence of diffuse atrial remodeling. Circulation. 2004; 109:1514–1522. [PubMed: 15007004]
17. Sasaki T, Miller CF, Hansford R, Yang J, Caffo BS, Zviman MM, Henrikson CA, Marine JE, Spragg D, Cheng A, Tandri H, Sinha S, Kolandaivelu A, Zimmerman SL, Bluemke DA, Tomaselli GF, Berger RD, Calkins H, Halperin HR, Nazarian S. Myocardial structural associations with local electrograms: a study of postinfarct ventricular tachycardia pathophysiology and magnetic resonance-based noninvasive mapping. Circ Arrhythm Electrophysiol. 2012; 5:1081–1090. [PubMed: 23149263]
18. Sasaki T, Miller CF, Hansford R, Zipunnikov V, Zviman MM, Marine JE, Spragg D, Cheng A, Tandri H, Sinha S, Kolandaivelu A, Zimmerman SL, Bluemke DA, Tomaselli GF, Berger RD, Halperin HR, Calkins H, Nazarian S. Impact of nonischemic scar features on local ventricular electrograms and scar-related ventricular tachycardia circuits in patients with nonischemic cardiomyopathy. Circ Arrhythm Electrophysiol. 2013; 6:1139–1147. [PubMed: 24235267]
19. Spragg DD, Khurram I, Zimmerman SL, Yarmohammadi H, Barcelon B, Needleman M, Edwards D, Marine JE, Calkins H, Nazarian S. Initial experience with magnetic resonance imaging of atrial scar and co-registration with electroanatomic voltage mapping during atrial fibrillation: success and limitations. Heart Rhythm. 2012; 9:2003–2009. [PubMed: 23000671]
20. Xu J, Cui G, Esmailian F, Plunkett M, Marelli D, Ardehali A, Odim J, Laks H, Sen L. Atrial extracellular matrix remodeling and the maintenance of atrial fibrillation. Circulation. 2004; 109:363–368. [PubMed: 14732752]
21. Rohr S. Myofibroblasts in diseased hearts: new players in cardiac arrhythmias? Heart Rhythm. 2009; 6:848–856. [PubMed: 19467515]
22. Rucker-Martin C, Pecker F, Godreau D, Hatem SN. Dedifferentiation of atrial myocytes during atrial fibrillation: role of fibroblast proliferation in vitro. Cardiovasc Res. 2002; 55:38–52. [PubMed: 12062707]
23. Yue L, Xie J, Nattel S. Molecular determinants of cardiac fibroblast electrical function and therapeutic implications for atrial fibrillation. Cardiovasc Res. 2011; 89:744–753. [PubMed: 20962103]
24. Spach MS, Dolber PC. Relating extracellular potentials and their derivatives to anisotropic propagation at a microscopic level in human cardiac muscle. Evidence for electrical uncoupling of side-to-side fiber connections with increasing age. Circ Res. 1986; 58:356–371. [PubMed: 3719925]
25. Rook MB, van Ginneken AC, de Jonge B, el Aoumari A, Gros D, Jongsma HJ. Differences in gap junction channels between cardiac myocytes, fibroblasts, and heterologous pairs. Am J Physiol. 1992; 263:C959–C977. [PubMed: 1279981]
26. Maleckar MM, Greenstein JL, Giles WR, Trayanova NA. Electrotonic coupling between human atrial myocytes and fibroblasts alters myocyte excitability and repolarization. Biophys J. 2009; 97:2179–2190. [PubMed: 19843450]
27. Krul SP, Berger WR, Smit NW, van Amersfoorth SC, Driessen AH, van Boven WJ, Fiolet JW, van Ginneken AC, van der Wal AC, de Bakker JM, Coronel R, de Groot JR. Atrial Fibrosis and Conduction Slowing in the Left Atrial Appendage of Patients Undergoing Thoracoscopic Surgical Pulmonary Vein Isolation for Atrial Fibrillation. Circ Arrhythm Electrophysiol. 2015; 8:288–295. [PubMed: 25673630]
28. Hansson A, Holm M, Blomstrom P, Johansson R, Luhrs C, Brandt J, Olsson SB. Right atrial free wall conduction velocity and degree of anisotropy in patients with stable sinus rhythm studied during open heart surgery. Eur Heart J. 1998; 19:293–300. [PubMed: 9519324]
29. Klos M, Calvo D, Yamazaki M, Zlochiver S, Mironov S, Cabrera JA, Sanchez-Quintana D, Jalife J, Berenfeld O, Kalifa J. Atrial septopulmonary bundle of the posterior left atrium provides a substrate for atrial fibrillation initiation in a model of vagally mediated pulmonary vein

tachycardia of the structurally normal heart. Circ Arrhythm Electrophysiol. 2008; 1:175–183. [PubMed: 19609369]

30. Platonov PG. Interatrial conduction in the mechanisms of atrial fibrillation: from anatomy to cardiac signals and new treatment modalities. Europace. 2007; 9(Suppl 6):vi10–vi16. [PubMed: 17959684]
31. Roberts DE, Hersh LT, Scher AM. Influence of cardiac fiber orientation on wavefront voltage, conduction velocity, and tissue resistivity in the dog. Circ Res. 1979; 44:701–712. [PubMed: 428066]
32. De PR, Ho SY, Salerno-Uriarte JA, Tritto M, Spadacini G. Electroanatomic analysis of sinus impulse propagation in normal human atria. J Cardiovasc Electrophysiol. 2002; 13:1–10. [PubMed: 11843475]
33. Ho SY, Sanchez-Quintana D, Cabrera JA, Anderson RH. Anatomy of the left atrium: implications for radiofrequency ablation of atrial fibrillation. J Cardiovasc Electrophysiol. 1999; 10:1525–1533. [PubMed: 10571372]
34. Wang K, Ho SY, Gibson DG, Anderson RH. Architecture of atrial musculature in humans. Br Heart J. 1995; 73:559–565. [PubMed: 7626357]
35. Poveda F, Gil D, Marti E, Andaluz A, Ballester M, Carreras F. Helical structure of the cardiac ventricular anatomy assessed by diffusion tensor magnetic resonance imaging with multiresolution tractography. Rev Esp Cardiol (Engl Ed). 2013; 66:782–790. [PubMed: 24773858]

WHAT IS KNOWN

- Regional left atrial late gadolinium enhancement heterogeneity has been noted on magnetic resonance imaging of patients with atrial fibrillation.
- The extent of left atrial late gadolinium enhancement appears to be associated with atrial fibrillation persistence and failure of pulmonary vein isolation for arrhythmia suppression.

WHAT THE STUDY ADDS

- Left atrial regions, which exhibit late gadolinium enhancement, exhibit lower local conduction velocity.
- Conduction velocity heterogeneity may mediate the association of late gadolinium enhancement with atrial fibrillation persistence and recurrence following pulmonary vein isolation.

A

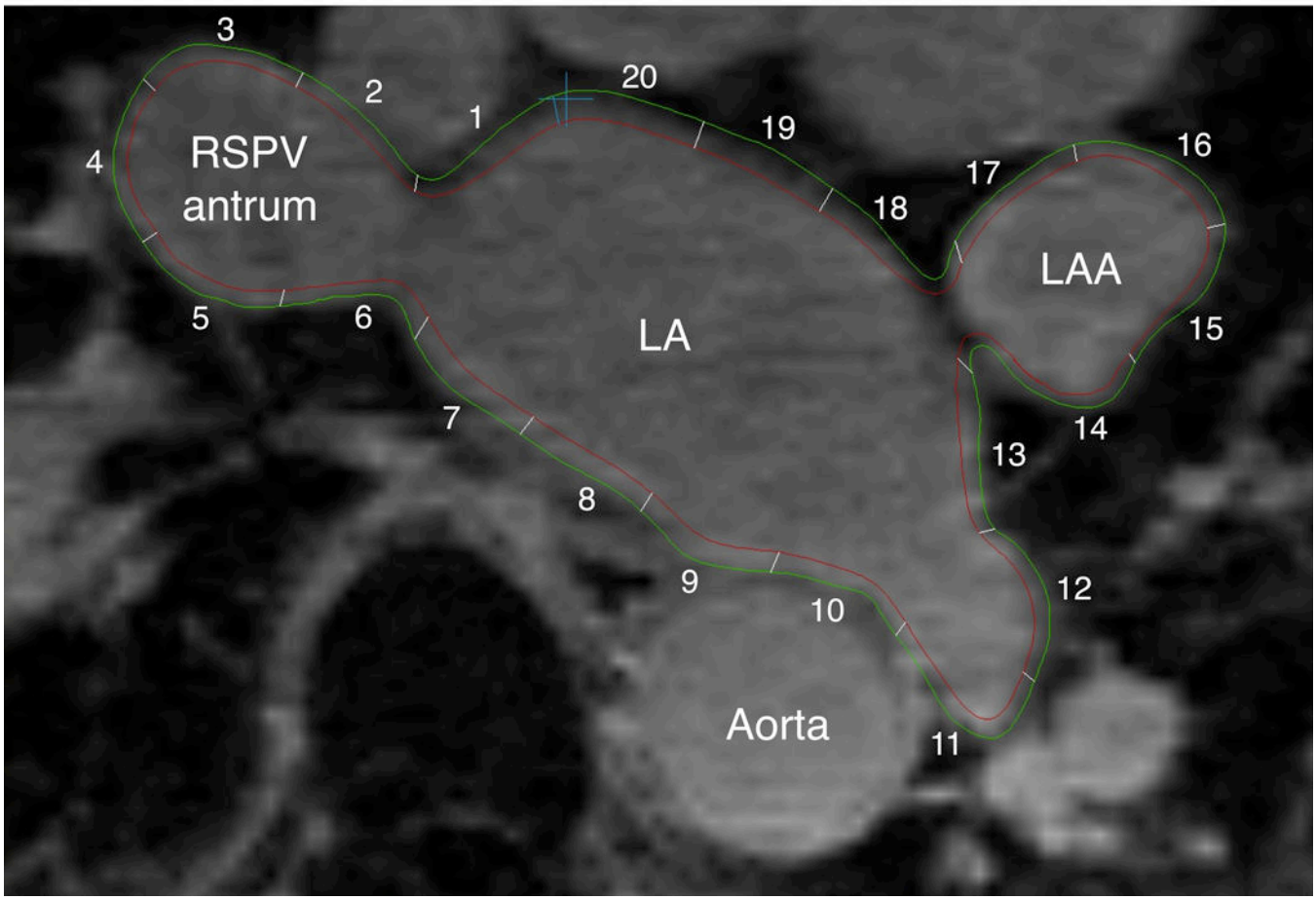

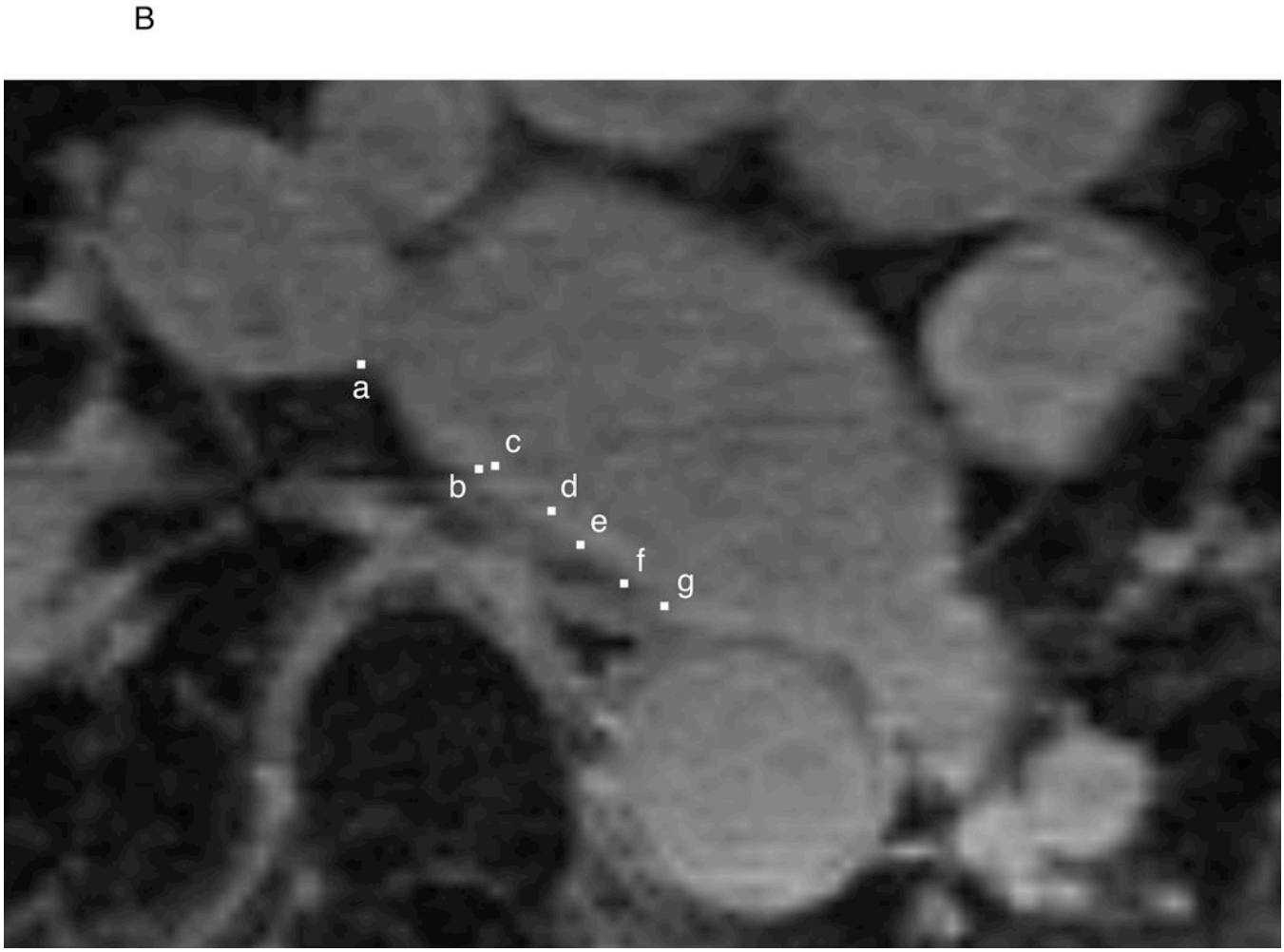

Figure 1.

Endocardial and epicardial LA contours and registration of EAM data to LGE-MRI in a representative case. **A:** The endocardial (red) and epicardial (green) contours were drawn on LGE-MRI axial planes. LA myocardium between the two contours was divided into 20 sectors and the mean pixel intensity and wall thickness of each sector were calculated. **B:** Location data of EAM (white square dots) were registered to the MRI by using custom software. In this example, EAM points a, b, c, d, e, f, and g correspond to the sectors 6, 7, 7, 8, 8, 9, and 9, respectively. LAA = left atrial appendage, RSPV = right superior pulmonary vein

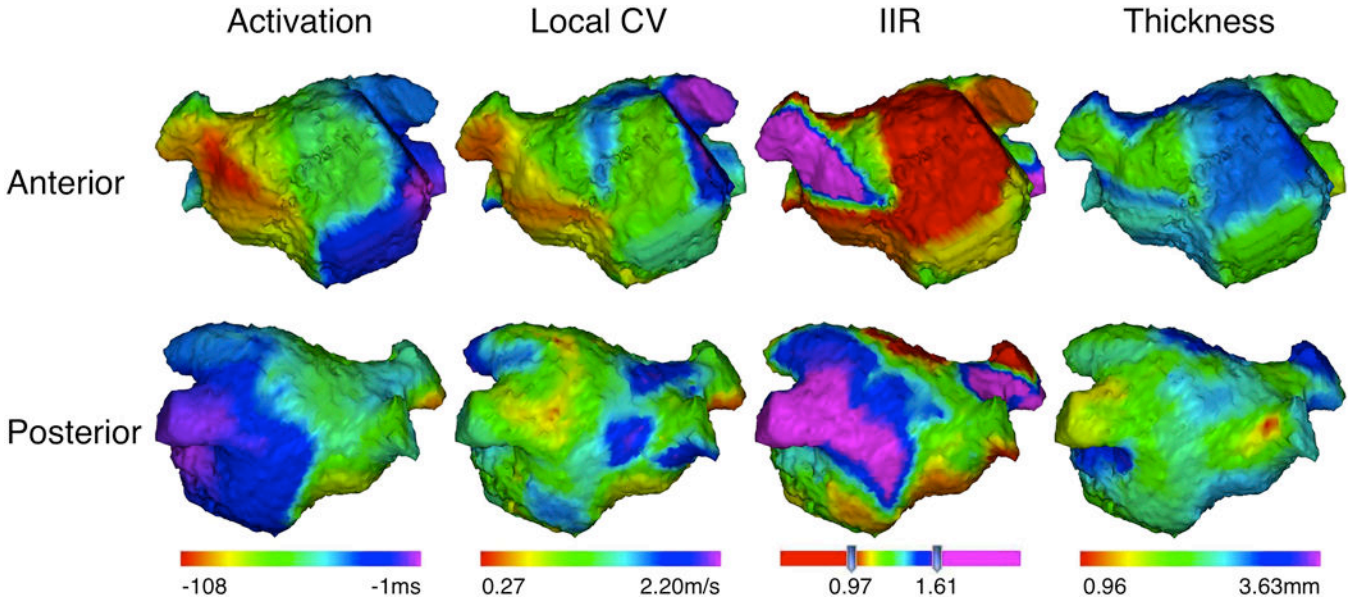

Figure 2.

Three-dimensional maps in a representative case. The upper and lower panels show the anterior and posterior projections of three-dimensional LA images merged with the data of local activation time, local CV, IIR, and wall thickness, respectively. Left atrial appendage was excluded from the figures.

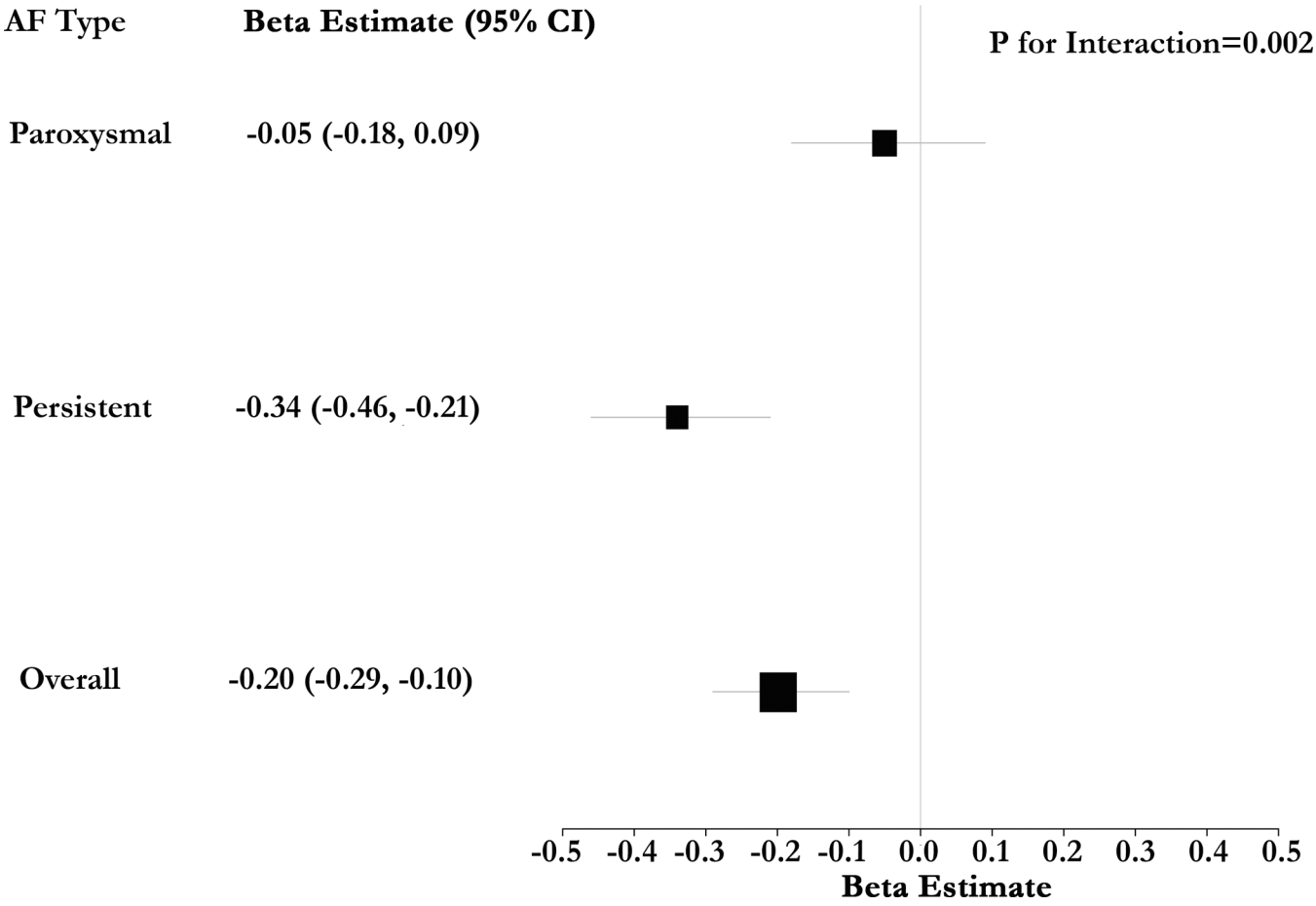

Figure 3.

Forest Plot of Beta Estimates for the Association of IIR with CV – The forest plot summarizes multivariable-adjusted beta estimates for the association of IIR with CV. Models were clustered by patient and adjusted for regional thickness. The association of IIR with CV was accentuated in patients with persistent AF. In contrast, while the direction of association was consistent, the magnitude of association was lower and statistical significance was absent in the subgroup with paroxysmal AF.

Table 1

Patient characteristics (N = 22)

Age (years)	62±9.0
Male	17 (77%)
BMI	29±5.8
Type of AF	
Paroxysmal	13 (59%)
Persistent	9 (41%)
AF duration (years)	4±4.5
LVEF (%)	61±4.2
CHA_2DS_2-VASc	1.9±1.8
Duration from preoperative MRI to ablation (days)	Median 1, limit 0–9

Data are presented as mean ± standard deviation, N (%), or median and limit.

BMI: body mass index
LVEF: left ventricular ejection fraction